

Effect of anisotropy on universal transport in unconventional superconductors

W. C. Wu

Department of Physics, National Taiwan Normal University, Taipei 11718, Taiwan

D. Branch and J. P. Carbotte

*Department of Physics and Astronomy, McMaster University
Hamilton, Ontario, Canada L8S 4M1*

(August 12, 2018)

We investigate the universal electronic transport for a mixed $d_{x^2-y^2}+s$ -wave superconductor in the presence of an anisotropic elliptical Fermi surface. Similar to the universal low-temperature transport predicted in a $d_{x^2-y^2}$ -wave superconductor with a circular Fermi surface, anisotropic universal features are found in the low-temperature microwave conductivity, and thermal conductivity in the anisotropic system. The effects of anisotropy on the penetration depth, impurity induced T_c suppression, and the zero-frequency density of states are also considered. While a small amount of anisotropy can lead to a strong suppression of the effective scattering rate and hence the density of states at zero frequency, experimental data suggests that large effects are restored by a negative s -component gap admixture.

PACS numbers: 78.30.-j, 74.62.Dh, 74.25.Gz

I. INTRODUCTION

It is well known that in high-temperature superconductors, owing to their layered nature and their reduced dimensionality, there exists significant anisotropy between various properties parallel and perpendicular to the copper oxide layers [1]. In some materials such as YBCO, anisotropy is also seen between properties along the a and b axes. These in-plane anisotropies are due to the presence of a CuO chain layer in addition to the CuO₂ plane layers. Thus the overall band structure parallel to the layer is orthorhombic instead of tetragonal. On the other hand, the symmetry of the superconducting gap remains controversial in high- T_c compounds. It is generally believed to be $d_{x^2-y^2}$ -wave, while many suggest that there is an additional s -wave component [2–5].

For a superconductor with order parameter with nodes on the Fermi surface, it is known that impurity scattering can lead to a finite density of quasiparticle states at zero energy (gapless excitations). As a consequence, while the effective impurity scattering rate γ is quite different for different impurity concentrations and different scattering limits, the in-plane microwave conductivity saturates at low temperatures and is independent of γ (or the impurity concentration). This universal transport phenomenon was first predicted by Lee [6] for a $d_{x^2-y^2}$ -wave superconductor. Later Graf *et al.* [7] found a similar universality in the thermal conductivity which is related to the microwave conductivity via the Wiedemann-Franz law. Recent thermal conductivity experiments done by Taillefer *et al.* [8] have confirmed these universal features. More recently, Wu and Carbotte [9] demonstrated how one can also study these universal features by doing channel-dependent Raman scattering experiments. It was found, in a $d_{x^2-y^2}$ -wave superconductor, that the low-temperature slope of the Raman intensity at zero

frequency are universal in the A_{1g} and B_{2g} channels, but strongly dependent on the scattering rate ($\sim \gamma^2$) in the B_{1g} channel [9].

The saturation of the low-temperature transport in an unconventional superconductor is a result of a cancellation between the value of the impurity-induced density of states at zero energy and the quasiparticle relaxation lifetime. It thus arises only if there exists nodes in the order parameter on the Fermi surface. In this paper, we consider the orthorhombic nature of the crystal structure in YBCO and explore whether an anisotropic universality exists in such a system. For simplicity, we study a system with an elliptical Fermi surface (assuming that the effective masses are different along x and y directions). We have simultaneously considered a $d_{x^2-y^2}$ -wave gap with an additional s -wave component. We investigate various quantities, including the in-plane low-temperature microwave conductivity, thermal conductivity, and the London penetration depth. It will be shown that a small amount of anisotropy (the combined contribution from energy band anisotropy and gap symmetry anisotropy) can lead to a drastic change in the effective scattering rate in the superconducting state. As a consequence, the system exhibits an anisotropic universal feature in various transport quantities. More interestingly, experimental data [10,11] seems suggesting that the effect of the large energy band anisotropy is largely compensated for by a *negative* s -wave component distortion to the $d_{x^2-y^2}$ -wave gap.

The content of this paper is as follows. In Sec. II, we establish the Kubo formalism needed for subsequent calculations. In Sec. III, we present our starting anisotropic model for a $d_{x^2-y^2}+s$ -wave superconductor with an orthorhombic elliptical Fermi surface. In Sec. IV, the anisotropic universal microwave conductivity, anisotropic magnetic penetration depth, and anisotropic universal

thermal conductivity are presented. In Sec. V, we discuss how the effective scattering rate and hence the density of states at zero frequency are modified in such an anisotropic system. The effect of anisotropy on the impurity-induced T_c suppression is also considered. A short conclusion is given in Sec. VI.

II. BASIC FORMALISM

We derive first the formalism for the optical conductivity in details. The microwave conductivity and the London penetration follow and are given by the real and imaginary parts of the optical conductivity in the limit of zero frequency. Later we will briefly derive the formalism for the thermal conductivity which shares a great similarity with that of the optical conductivity.

The optical conductivity is given by [12]

$$\sigma_{\mu\nu}(\Omega) = \frac{i}{\Omega} \left[K_{\mu\nu}(\mathbf{q} \rightarrow 0, i\nu_n \rightarrow \Omega + i\delta) - K_{\mu\nu}^{(n)}(\mathbf{q} \rightarrow 0, 0) \right], \quad (1)$$

where $K_{\mu\nu}$ is the paramagnetic Kubo function given by

$$K_{\mu\nu}(\mathbf{q}, i\nu_n) = \frac{e^2 T}{2} \sum_{\mathbf{k}, \omega_n} \quad (2)$$

$$\text{Tr} \left[\hat{\gamma}_\mu(\mathbf{k} + \frac{\mathbf{q}}{2}) \hat{G}(\mathbf{k}, i\omega_n + i\nu_n) \hat{\gamma}_\nu(\mathbf{k} + \frac{\mathbf{q}}{2}) \hat{G}(\mathbf{k} + \mathbf{q}, i\omega_n) \right],$$

with Tr denoting a trace. In Eq. (1), the second term $K_{\mu\nu}^{(n)}$ is calculated in the normal state and with a minus sign corresponds to a diamagnetic response. The current vertex in Eq. (2) is given by

$$\hat{\gamma}_\mu(\mathbf{k}) = \frac{1}{\hbar} \frac{\partial \xi_{\mathbf{k}}}{\partial k_\mu} \hat{\tau}_0, \quad (3)$$

with $\hat{\tau}_i$'s the Pauli matrices and $\xi_{\mathbf{k}}$ the electronic dispersion relation of the superconducting layer. In Eq. (2), we have ignored the contribution to the vertex corrections due to the impurity potentials and superconducting two-particle pairing interactions. For isotropic impurity scattering, it is sufficient to use the bubble diagram at small \mathbf{q} , while the inclusion of the pairing interaction vertex correction is negligible at the low frequencies of interest. However, the effect of impurities is fully included in the single-particle matrix Green's function \hat{G} in Eq. (2).

In terms of the particle-hole space, the single-particle matrix Green's function is given by

$$\hat{G}(\mathbf{k}, i\omega_n) = \frac{i\tilde{\omega}_n \hat{\tau}_0 + \tilde{\xi}_{\mathbf{k}} \hat{\tau}_3 + \tilde{\Delta}_{\mathbf{k}} \hat{\tau}_1}{(i\tilde{\omega}_n)^2 - \tilde{\xi}_{\mathbf{k}}^2 - \tilde{\Delta}_{\mathbf{k}}^2} \quad (4)$$

where $\tilde{\omega}_n$, $\tilde{\xi}_{\mathbf{k}}$, and $\tilde{\Delta}_{\mathbf{k}}$ are the impurity-renormalized Matsubara frequencies, electron energy spectrum, and gap. \hat{G} is related to the noninteracting Green's function $\hat{G}_0^{-1}(\mathbf{k}, i\omega_n) = i\omega_n \hat{\tau}_0 - \xi_{\mathbf{k}} \hat{\tau}_3 - \Delta_{\mathbf{k}} \hat{\tau}_1$ via the Dyson's equation

$$\hat{G}^{-1}(\mathbf{k}, i\omega_n) = \hat{G}_0^{-1}(\mathbf{k}, i\omega_n) - \hat{\Sigma}(\mathbf{k}, i\omega_n). \quad (5)$$

We shall solve the self-energy $\hat{\Sigma}$ due to the impurity scattering. By expanding $\hat{\Sigma}(\mathbf{k}, i\omega_n) \equiv \sum_{\alpha} \Sigma_{\alpha}(\mathbf{k}, i\omega_n) \hat{\tau}_{\alpha}$

($\alpha = 0, 1, 3$), one finds $i\tilde{\omega}_n = i\omega_n - \Sigma_0$, $\tilde{\xi}_{\mathbf{k}} = \xi_{\mathbf{k}} + \Sigma_3$, and $\tilde{\Delta}_{\mathbf{k}} = \Delta_{\mathbf{k}} + \Sigma_1$. Employing the usual T -matrix approximation, the self-energy is then given by $\hat{\Sigma}(\mathbf{k}, i\omega_n) = n_i \hat{T}(\mathbf{k}, \mathbf{k}, i\omega_n)$, where n_i is the impurity density and

$$\begin{aligned} \hat{T}(\mathbf{k}, \mathbf{k}', i\omega_n) &= v_i(\mathbf{k}, \mathbf{k}') \hat{\tau}_3 \\ &+ \sum_{\mathbf{k}''} v_i(\mathbf{k}, \mathbf{k}'') \hat{\tau}_3 \hat{G}(\mathbf{k}'', i\omega_n) \hat{T}(\mathbf{k}'', \mathbf{k}', i\omega_n). \end{aligned} \quad (6)$$

Here $v_i(\mathbf{k}, \mathbf{k}') \equiv \langle \mathbf{k}' | v_i | \mathbf{k} \rangle$ is the impurity potential. If we consider only isotropic impurity scattering [$v_i(\mathbf{k}, \mathbf{k}') = v_i$], the T -matrix in (6) is left only with frequency dependence and can be solved to get

$$\hat{T}(i\omega_n) = \left[1 - v_i \hat{\tau}_3 \hat{\tilde{G}}(i\omega_n) \right]^{-1} v_i \hat{\tau}_3 \quad (7)$$

with the integrated Green's function $\hat{\tilde{G}}(i\omega_n) \equiv \sum_{\mathbf{k}} \hat{G}(\mathbf{k}, i\omega_n)$. One can expand $\hat{\tilde{G}}(i\omega_n) = \sum_{\alpha} G_{\alpha}(i\omega_n) \hat{\tau}_{\alpha}$ ($\alpha = 0, 1, 3$) with $G_{\alpha}(i\omega_n) \equiv 1/2 \sum_{\mathbf{k}} \text{Tr}[\hat{\tau}_{\alpha} \hat{G}(\mathbf{k}, i\omega_n)]$. For a superconductor with particle-hole symmetry, $G_3(i\omega_n) = 0$ and one obtains

$$\begin{aligned} \Sigma_0(i\omega_n) &= \frac{n_i G_0(i\omega_n)}{c^2 - G_0^2(i\omega_n) + G_1^2(i\omega_n)} \\ \Sigma_1(i\omega_n) &= \frac{-n_i G_1(i\omega_n)}{c^2 - G_0^2(i\omega_n) + G_1^2(i\omega_n)} \\ \Sigma_3(i\omega_n) &= \frac{cn_i}{c^2 - G_0^2(i\omega_n) + G_1^2(i\omega_n)}, \end{aligned} \quad (8)$$

where $c^2 \equiv 1/v_i^2$. The effect of Σ_3 is usually absorbed into the chemical potential and consequently $\tilde{\xi}_{\mathbf{k}} \equiv \xi_{\mathbf{k}}$ or $\Sigma_3 \equiv 0$. It is noted that for a system with a cylindrical Fermi surface and a pure d -wave gap, $G_1 = 0$ and hence $\Sigma_1 = 0$ which gives no renormalization effect on the gap ($\tilde{\Delta}_{\mathbf{k}} = \Delta_{\mathbf{k}}$). However, our present interest is to include this renormalization effect for an elliptical Fermi surface system and gap with a possible s -component appropriate to an orthorhombic system. The Green's function (4) and above self-energies are solved self-consistently along with the gap equation

$$\Delta_{\mathbf{k}} = \frac{T}{2} \sum_{\mathbf{k}', \omega_n} g(\mathbf{k}, \mathbf{k}') \text{Tr}[\hat{\tau}_1 \hat{G}(\mathbf{k}', i\omega_n)], \quad (9)$$

where $g(\mathbf{k}, \mathbf{k}')$ is the pairing interaction.

III. ANISOTROPIC MODEL

We consider a layered superconductor of a $d_{x^2-y^2} + s$ -wave order parameter

$$\Delta_{\mathbf{k}} = \Delta_0(\hat{k}_x^2 - \hat{k}_y^2 + s), \quad (10)$$

where the constant s denotes the s -wave component which is small but can be *positive* or *negative* in general. For YBCO which is orthorhombic, the band structure is chosen to be elliptical

$$\xi(k_x, k_y) = \frac{\hbar^2 k_x^2}{2m_x} + \frac{\hbar^2 k_y^2}{2m_y} - \epsilon_F, \quad (11)$$

where ϵ_F is the Fermi energy and taking into account the CuO chain along the k_y axis, the effective mass $m_x > m_y$. Our approach follows Kim and Nicol [13] closely. It is convenient to use a transformation

$$k_\mu \equiv p_\mu \sqrt{\frac{2m_\mu}{m_x + m_y}}; \quad (\mu = x, y) \quad (12)$$

and consequently Eqs. (10) and (11) are transformed from the \mathbf{k} frame to \mathbf{p} frame according to

$$\Delta_{\mathbf{k}} \rightarrow \Delta_{\mathbf{p}} = \Delta_0 f(\phi) \quad (13)$$

with

$$f(\phi) = \frac{\cos(2\phi) + \alpha}{1 + \alpha \cos(2\phi)} + s; \quad \alpha \equiv \frac{m_x - m_y}{m_x + m_y} > 0 \quad (14)$$

and

$$\xi(k_x, k_y) \rightarrow \xi(p_x, p_y) = \frac{\hbar^2}{m_x + m_y} (p_x^2 + p_y^2) - \epsilon_F. \quad (15)$$

The denominator in (14) was ignored in the work of Kim and Nicol [13]. In (13), ϕ denotes the azimuthal angle in the \mathbf{p} frame. The cylindrical Fermi surface case corresponds to $m_x = m_y$ or $\alpha = 0$. It is worth noting that the gap given in (13) viewed from the \mathbf{p} frame is not a simple $d+s$ -wave gap, $\Delta_{\mathbf{p}} = \Delta_0(\cos(2\phi) + s)$, unless $\alpha = 0$. Fig. 1 displays the gaps given by (13) and (14) with various choice of α and s . The general feature of these pictures is that the gap nodes are shifted off the diagonals and for the case $\alpha = -s$, the nodes are pushed back to the diagonal. These are to be compared by the pure d -wave case ($\alpha = s = 0$) case.

The momentum \mathbf{k} sum can be transformed to \mathbf{p} sum which in turn can be replaced by an integration

$$\sum_{\mathbf{k}} \rightarrow \sum_{\mathbf{p}} = 2N(0) \int_{-\infty}^{\infty} d\xi_{\mathbf{p}} \int_0^{2\pi} \frac{d\phi}{2\pi}, \quad (16)$$

with $N(0) = (m_x + m_y)/4\pi\hbar^2$ defined as the density of states per spin on the Fermi surface in \mathbf{p} frame. In the normal state in which $\Delta_{\mathbf{k}} = 0$ and hence $G_1 = \Sigma_1 = 0$, the only nontrivial self-energy in (8) is $\Sigma_0 = n_i G_0/(c^2 - G_0^2)$. Using (16), one can easily work out the (isotropic) scattering rate $i\Sigma_0 \equiv (1/2\tau)$, where in the Born scattering ($c \gg 1$) limit, $1/2\tau = 2\pi N(0)n_i v_i^2$, while in the resonant scattering ($c \ll 1$) limit, $1/2\tau = n_i/2\pi N(0)$.

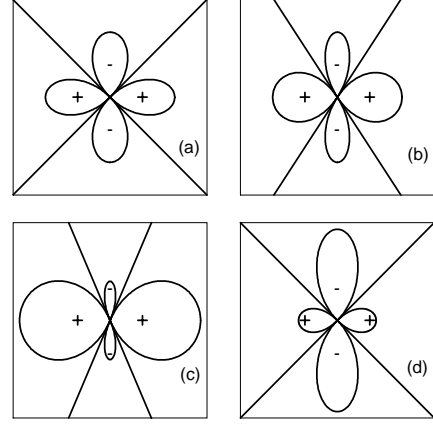


FIG. 1. Order parameters on the Fermi surface given by Eq. (13). (a): $\alpha = s = 0$ (pure d -wave gap); (b): $\alpha = 0.4$, $s = 0$; (c): $\alpha = 0.4$, $s = 0.4$; (d): $\alpha = 0.4$, $s = -0.4$. The straight lines denote the nodal angles.

Using the spectral representation for the imaginary frequency Green's function, analytically continuing to real frequency from imaginary frequency ($i\omega_n \rightarrow \omega + i\delta$), and then performing the frequency sum and momentum sum gives the real part of the Kubo function

$$K'_{\mu\nu}(\Omega) = \frac{N(0)e^2}{2} \int_0^{2\pi} \frac{d\phi}{2\pi} \gamma_\mu(\phi) \gamma_\nu(\phi) \int_{-\infty}^{\infty} d\omega \times \{ [f(\omega) - f(\omega - \Omega)] \text{Re} I_{+-}(\Omega, \omega) - [f(\omega) + f(\omega - \Omega)] \text{Re} I_{++}(\Omega, \omega) \} \quad (17)$$

and the imaginary part of the Kubo function

$$K''_{\mu\nu}(\Omega) = -\frac{N(0)e^2}{2} \int_0^{2\pi} \frac{d\phi}{2\pi} \gamma_\mu(\phi) \gamma_\nu(\phi) \int_{-\infty}^{\infty} d\omega \times [f(\omega) - f(\omega - \Omega)] [\text{Im} I_{+-}(\Omega, \omega) + \text{Im} I_{++}(\Omega, \omega)]. \quad (18)$$

In Eqs. (17) and (18), the vertices calculated on the Fermi surface are $\gamma_x(\phi) = \sqrt{2\epsilon_F/m_x} \cos \phi$ and $\gamma_y(\phi) = \sqrt{2\epsilon_F/m_y} \sin \phi$ and we have defined

$$I_{++}(\Omega, \omega) = -\frac{1}{\xi_+} + \frac{\tilde{\omega}'_+(\tilde{\omega}_+ + \tilde{\omega}'_+) + \tilde{\Delta}'_+(\tilde{\Delta}_+ - \tilde{\Delta}'_+)}{(\xi_+ + \xi'_+)\xi_+\xi'_+}, \\ I_{+-}(\Omega, \omega) = \frac{1}{\xi_+} + \frac{\tilde{\omega}'_-(\tilde{\omega}_+ + \tilde{\omega}'_-) + \tilde{\Delta}'_-(\tilde{\Delta}_+ - \tilde{\Delta}'_-)}{(\xi_+ - \xi'_+)\xi_+\xi'_-}, \quad (19)$$

with $\tilde{\omega}_\pm \equiv i\tilde{\omega}_n(\omega \pm i\delta)$; $\tilde{\omega}'_\pm \equiv i\tilde{\omega}_n(\omega - \Omega \pm i\delta)$, $\tilde{\Delta}_\pm \equiv \tilde{\Delta}(\omega \pm i\delta)$; $\tilde{\Delta}'_\pm \equiv \tilde{\Delta}(\omega - \Omega \pm i\delta)$, and $\xi_\pm \equiv \text{sgn}(\omega) \sqrt{\tilde{\omega}_\pm^2 - \tilde{\Delta}_\pm^2}$; $\xi'_\pm \equiv \text{sgn}(\omega - \Omega) \sqrt{(\tilde{\omega}'_\pm)^2 - (\tilde{\Delta}'_\pm)^2}$ which are chosen to have branch cuts such that $\text{Im} \xi_+, \text{Im} \xi'_+ > 0$ and $\text{Im} \xi_-, \text{Im} \xi'_- < 0$. The results of Eq. (17)-(19) were obtained before by Hirschfeld *et al.* [14] and many others. The microwave conductivity is given directly by $K''_{\mu\nu}$ as

$$\sigma_{\mu\nu}(T) = \lim_{\Omega \rightarrow 0} -\frac{K''_{\mu\nu}(\Omega, T)}{\Omega}, \quad (20)$$

while the London penetration depth is given via $K'_{\mu\nu}$ as

$$\frac{1}{\lambda_{\mu\nu}^2(T)} = \frac{4\pi}{c^2} \left[K'_{\mu\nu}(\Omega = 0, T) - K'^{(n)}_{\mu\nu}(\Omega = 0, T) \right], \quad (21)$$

with c the speed of light.

IV. ANISOTROPIC UNIVERSAL TRANSPORTS

A. Microwave Conductivity

We consider the zero-temperature limit of the microwave conductivity. When $T \rightarrow 0$, $[f(\omega) - f(\omega - \Omega)]/\Omega \approx \partial f(\omega)/\partial \omega \approx -\delta(\omega)$ as $\Omega \rightarrow 0$. Consequently from (18) and (20), we have

$$\sigma_{\mu\nu}(0) = N(0)e^2 \left\langle \frac{\gamma_\mu(\phi)\gamma_\nu(\phi)\gamma^2}{[\gamma^2 + \tilde{\Delta}^2(\phi)]^{\frac{3}{2}}} \right\rangle, \quad (22)$$

where $\langle \cdot \rangle$ denotes an average over the Fermi surface. In (22), $\gamma = -i\tilde{\omega}(\omega = 0) = i\Sigma_0(\omega = 0)$ and $\tilde{\Delta}(\phi) \equiv \tilde{\Delta}(\phi, \omega = 0) = \Delta_0[f(\phi) + \delta]$ with $\delta = \Sigma_1(\omega = 0)/\Delta_0$, respectively are the impurity-renormalized effective scattering rate and gap at zero frequency. For $\delta \ll 1$ and $\alpha + s < 1$ of interest [see Eq. (14)], it is guaranteed that there exists nodes for the renormalized gap. The appearance of universal transport in unconventional superconductors is intimately connected to the presence of nodes in the renormalized gap. When the anisotropies vanish ($\alpha = s = 0$), $f(\phi) = \cos(2\phi)$ and $\delta = 0$ which are correct whatever concentration of impurity and correspond to the unrenormalized pure d -wave gap in a cylindrical Fermi surface case. We will discuss in the next section, the self-consistent results for γ and δ in the two different scattering limits, Born and resonant.

In the case $\tilde{\gamma} \equiv \gamma/\Delta_0 \ll 1$, the major contribution to the average in Eq. (22) comes from the small angular area around the nodes of the renormalized gap. One can then carry out the integration in (22) to get

$$\sigma_{\nu\nu}(0) \simeq \frac{4N(0)e^2}{\pi\Delta_0} \left| \frac{\partial f(\phi)}{\partial \phi} \right|_{\phi=\phi_0}^{-1} \gamma_\nu(\phi_0)\gamma_\nu(\phi_0), \quad (23)$$

where ϕ_0 corresponds to the angle of nodes, *i.e.*, $f(\phi_0) = -\delta$. The cross term $\sigma_{xy}(0) = 0$ because of the Fermi-surface average. More explicitly, Eq. (23) gives

$$\begin{aligned} \sigma_{xx}(0) &= \frac{2e^2\epsilon_F N(0)}{\pi\Delta_0 m_x} \frac{(1 + \alpha\eta)^2(1 + \eta)}{\sqrt{1 - \eta^2(1 - \alpha^2)}}, \\ \sigma_{yy}(0) &= \frac{2e^2\epsilon_F N(0)}{\pi\Delta_0 m_y} \frac{(1 + \alpha\eta)^2(1 - \eta)}{\sqrt{1 - \eta^2(1 - \alpha^2)}}, \end{aligned} \quad (24)$$

where we have defined $\eta \equiv \cos(2\phi_0) = -(\alpha + s + \delta)/[1 + \alpha(s + \delta)]$. One can easily verify that when $\alpha = s = 0$ and

hence $\delta = 0$ corresponding to a $d_{x^2-y^2}$ -wave gap in the cylindrical Fermi surface case ($m_x = m_y$),

$$\sigma_{xx}(0) = \sigma_{yy}(0) = \frac{ne^2}{\pi\Delta_0 m}, \quad (25)$$

with $n = k_F^2/2\pi$ for the electronic density. The universal feature of (25) was first predicted by Lee [6].

While the result in Eq. (24) does not depend on γ , it is explicitly dependent of the gap shift δ which in turn, is associated with the impurity concentration. In the large resulting anisotropy case $[(\alpha + s)^2 \gg 1/(\tau\Delta_0)]$ of primary interest (provided the impurity concentration is low), one can ignore δ (compared to α and s) in Eq. (24), valid for both Born and unitary limits (see Sec. V). As a consequence,

$$\begin{aligned} \sigma_{xx}(0) &= \frac{2e^2\epsilon_F N(0)}{\pi\Delta_0} \frac{A_{xx}}{m_x} \equiv \frac{\Omega_{p,xx}^2}{4\pi} \frac{A_{xx}}{\pi\Delta_0} \\ \sigma_{yy}(0) &= \frac{2e^2\epsilon_F N(0)}{\pi\Delta_0} \frac{A_{yy}}{m_y} \equiv \frac{\Omega_{p,yy}^2}{4\pi} \frac{A_{yy}}{\pi\Delta_0}, \end{aligned} \quad (26)$$

where we have defined

$$\begin{aligned} A_{xx} &= \frac{1 - \alpha^2}{(1 + \alpha s)^2} \frac{(1 - \alpha - s + \alpha s)}{\sqrt{1 - \alpha^2 - s^2 + \alpha^2 s^2}}, \\ A_{yy} &= \frac{1 - \alpha^2}{(1 + \alpha s)^2} \frac{(1 + \alpha + s + \alpha s)}{\sqrt{1 - \alpha^2 - s^2 + \alpha^2 s^2}}. \end{aligned} \quad (27)$$

In (26), $\Omega_{p,xx}(\Omega_{p,yy})$ is the plasma frequency in the $x(y)$ direction [15,16]. In comparison with experiment, the plasma frequency is a measured quantity and so $\sigma_{ii}(0)$ is a measure of A_{ii}/Δ_0 . Note the extra factor of A_{ii} in (26) as compared with the well-known result (25) which is $\sigma(0) = (\Omega_p^2/4\pi)(1/\pi\Delta_0)$.

Eq. (26) represents the anisotropic universal feature in the microwave conductivity for an $d_{x^2-y^2}+s$ -wave superconductor with an orthorhombic band structure. The ratio

$$\frac{\sigma_{xx}(0)}{\sigma_{yy}(0)} = \frac{\Omega_{p,xx}^2}{\Omega_{p,yy}^2} \frac{A_{xx}}{A_{yy}} \quad (28)$$

should have some experimental consequence. We note that the low-temperature correction terms to $\sigma_{ii}(0)$ will be proportional to T^2/γ^2 with γ the effective impurity scattering rate. Thus when $T \ll \gamma$, the anisotropic universal values can be attained.

In the small anisotropy case $[(\alpha + s)^2 \ll 1/(\tau\Delta_0)]$, while α and $|s|$ may be large individually, it can be shown that $\delta \sim (\alpha + s) \sim \eta$ are all small (see Sec. V). Consequently, one ignores η in (24) to obtain

$$\begin{aligned} \sigma_{xx}(0) &= \frac{\Omega_{p,xx}^2}{4\pi^2\Delta_0(1 - \alpha^2)}, \\ \sigma_{yy}(0) &= \frac{\Omega_{p,yy}^2}{4\pi^2\Delta_0(1 - \alpha^2)}. \end{aligned} \quad (29)$$

A ratio $\sigma_{xx}(0)/\sigma_{yy}(0) = \Omega_{p,xx}^2/\Omega_{p,yy}^2$ is given in this limit. In the case of $\alpha \rightarrow 0$, $\sigma_{xx}(0) = \sigma_{yy}(0)$ in (29) and they reduce to Eq. (25).

B. London Penetration Depth

We consider here, the *anisotropic* London penetration depths within our anisotropic Fermi surface model together with a $d_{x^2-y^2}+s$ -wave order parameter. The results are to be compared to the recent work of Kim and Nicol [13] who effectively have considered the anisotropic penetration depth with $\alpha = 0$ because they ignore the denominator in (14). In the pure limit, using Eqs. (2) and (21) it can be shown that the square of the inverse penetration depth is given by

$$\frac{1}{\lambda_{\nu\nu}^2}(T) = \frac{8\pi e^2}{c^2} \frac{1}{\Omega} \sum_{\mathbf{k}} v_{\mathbf{k},\nu}^2 \left[\frac{\partial f(E_{\mathbf{k}})}{\partial E_{\mathbf{k}}} - \frac{\partial f(\epsilon_{\mathbf{k}})}{\partial \epsilon_{\mathbf{k}}} \right] \quad (30)$$

and is associated with the superfluid density. In the low-temperature limit, one obtains relatively simple results

$$\begin{aligned} \frac{1}{\lambda_{xx}^2}(T) &= \frac{\Omega_{p,xx}^2}{c^2} \left[1 - 2 \ln 2 \left(\frac{k_B T}{\Delta_0} \right) A_{xx} \right], \\ \frac{1}{\lambda_{yy}^2}(T) &= \frac{\Omega_{p,yy}^2}{c^2} \left[1 - 2 \ln 2 \left(\frac{k_B T}{\Delta_0} \right) A_{yy} \right], \end{aligned} \quad (31)$$

where A_{xx} and A_{yy} are given in Eq. (27).

Our result confirms Kim and Nicol's result when we set $\alpha = 0$. The linear in temperature behavior in Eq. (31) is expected for an unconventional superconductor with gap nodes on Fermi surface in the clean limit. When impurities are present, one instead expects a T^2 law for the low-temperature penetration depth (see Ref. [13]). In view of (31), the discrepancy exhibited in a and b -axis penetration depths can be studied in two ways. First, the zero-temperature anisotropic penetration depth ratio

$$\frac{\lambda_{yy}^2(0)}{\lambda_{xx}^2(0)} = \frac{\Omega_{p,xx}^2}{\Omega_{p,yy}^2} = \frac{m_y}{m_x} = \frac{1-\alpha}{1+\alpha}. \quad (32)$$

Secondly, the low-temperature slope ratio

$$\frac{d[\lambda_{xx}^2(0)/\lambda_{xx}^2(T)]/dT|_{T \rightarrow 0}}{d[\lambda_{yy}^2(0)/\lambda_{yy}^2(T)]/dT|_{T \rightarrow 0}} = \frac{A_{xx}}{A_{yy}}. \quad (33)$$

To fit the experimental data of low-temperature penetration depth by Bonn *et al.* [17] and the normal-state resistivity by Zhang *et al.* [18], it requires $\alpha = 0.4$ in (32) and then a value of $s = -0.25$ is obtained using (33) [19].

In Fig. 2, we plot the relative size of gap $\Delta(\phi)$ as a function of angle using parameters fit to low-temperature penetration depth slopes ($\alpha = 0.4$, $s = -0.25$). As shown in Fig. 2, the gap node is shifted from 45° and the overall gap magnitude is highly anisotropic. These may have observable consequence in future ARPES experiments.

C. Thermal Conductivity

In analogy to Eq. (18) which gives the microwave conductivity, the thermal conductivity is given by

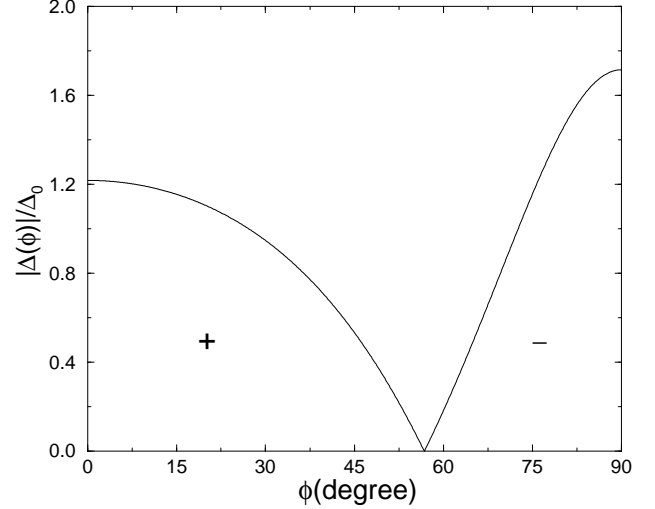


FIG. 2. Relative magnitude of order parameter [given by Eq. (13)] vs. angle using parameters fit to penetration depth low-temperature slopes ($\alpha = 0.4$ and $s = -0.25$).

$$\begin{aligned} \kappa_{\mu\nu}(T) &= -\frac{N(0)}{2T} \int_0^{2\pi} \frac{d\phi}{2\pi} \gamma_\mu(\phi) \gamma_\nu(\phi) \int_{-\infty}^{\infty} d\omega \omega^2 \frac{\partial f(\omega)}{\partial \omega} \\ &\times [\text{Im} I_{+-}(\Omega = 0, \omega) + \text{Im} I_{++}(\Omega = 0, \omega)]. \end{aligned} \quad (34)$$

As we seek the anisotropic universality in thermal conductivity, we are specifically interested in the $T \rightarrow 0$ regime in which the inelastic scattering is unimportant. When $T \rightarrow 0$, the ω integration in Eq. (34) is limited to $\omega \approx 0$ and consequently

$$\begin{aligned} \frac{\kappa_{\mu\nu}(T \rightarrow 0)}{\sigma_{\mu\nu}(T \rightarrow 0)} &= \frac{1}{T} \int_{-\infty}^{\infty} d\omega \omega^2 \frac{\partial f(\omega)}{\partial \omega} \bigg/ e^2 \int_{-\infty}^{\infty} dx \frac{\partial f(\omega)}{\partial \omega} \\ &= \frac{\pi^2}{3} \left(\frac{k_B}{e} \right)^2 T. \end{aligned} \quad (35)$$

Therefore the Wiedemann-Franz law (or Sommerfeld law) is satisfied. The above result is valid for both a and b directions. Previously Graf *et al.* [7] have shown that for an isotropic Fermi surface band structure, the thermal conductivity saturates and obeys the Wiedemann-Franz law at low temperatures ($T \ll \gamma$) for disordered gapless superconductors. As emphasized by Graf *et al.* [7], similar to the condition of universal microwave conductivity, the validity of the Wiedemann-Franz law at $T \rightarrow 0$ is a unique feature of gapless superconductors in which the impurity induces a finite density of states at the zero energy. Our predicted *anisotropic* universal thermal conductivity can be written explicitly as [when $(\alpha + s)^2 \gtrsim 1/(\tau \Delta_0)$]

$$\begin{aligned} \frac{\kappa_{xx}(T)}{T} \bigg|_{T \rightarrow 0} &= \frac{1}{12} \left(\frac{k_B}{e} \right)^2 \Omega_{p,xx}^2 \frac{A_{xx}}{\Delta_0} \\ \frac{\kappa_{yy}(T)}{T} \bigg|_{T \rightarrow 0} &= \frac{1}{12} \left(\frac{k_B}{e} \right)^2 \Omega_{p,yy}^2 \frac{A_{yy}}{\Delta_0}. \end{aligned} \quad (36)$$

Thus, similar to Eq. (28),

$$\frac{\kappa_{xx}(0)}{\kappa_{yy}(0)} = \frac{\Omega_{p,xx}^2}{\Omega_{p,yy}^2} \frac{A_{xx}}{A_{yy}}. \quad (37)$$

Recently, an experiment done by Taillefer *et al.* [8] which measures the in-plane low-temperature thermal conductivity of $\text{YBa}_2\text{Cu}_3\text{O}_{6.9}$ at different Zn substitutions for Cu has confirmed the universal feature in thermal conductivity. More recently, Chiao *et al.* [11] have observed the anisotropic universal thermal conductivity in YBCO. They found that the thermal conductivity saturates at low temperatures both along a and b directions from which an anisotropy $\kappa_b(T \rightarrow 0)/\kappa_a(T \rightarrow 0) = 1.3$ is obtained [11]. If we take $\alpha = 0.4$ as predicted by anisotropic in-plane penetration depth [17] and normal-state resistivity [18] data, it would imply a negative but large $s = -0.60$ in use of Eq. (37). Unfortunately such a large value of s reverses the order of the slopes in the penetration depth making the x direction steeper than the y direction in contradiction to experiment. For very small $1/\tau$, it can also imply a very small value of γ so that saturation effects will be seen only at very low temperature again in contradiction to experiment. On the other hand, with $\alpha = 0.4$ and $s = -0.60$, the value of $A_{xx} \simeq 1.9$ makes it unnecessary to invoke a factor of 2 in the slope of the gap at the nodes needed in the analysis of Taillefer *et al.* [8] who concluded that the actual gap grows out of zero a factor of 2 more slowly than in a pure d -wave case.

The large negative value of s needed to explain the observed small anisotropy between a and b direction in the thermal conductivity is not believed to be physical. A more likely explanation may be in the observation that even for pure crystals of optimally doped YBCO, there is a large residual resistivity on the chains and none on the planes. This highly anisotropic residual resistivity has not been accounted for in our work.

V. SELF-ENERGIES AND DENSITY OF STATES

We discuss here the self-consistent results for the dimensionless self-energies $\bar{\gamma}$ and δ . One recalls that $\bar{\gamma} = i\Sigma_0(\omega = 0)/\Delta_0$ and $\delta = \Sigma_1(\omega = 0)/\Delta_0$. The self-energies Σ_i in (8) are comprised of the integrated Green's functions G_i which are given by

$$G_0(\omega) = -2i\pi N(0) \left\langle \frac{\tilde{\omega}}{\sqrt{\tilde{\omega}^2 - \tilde{\Delta}^2(\phi, \omega)}} \right\rangle \quad (38)$$

and

$$G_1(\omega) = -2i\pi N(0) \left\langle \frac{\tilde{\Delta}(\phi, \omega)}{\sqrt{\tilde{\omega}^2 - \tilde{\Delta}^2(\phi, \omega)}} \right\rangle, \quad (39)$$

after the energy integration is done. For the case $\delta, \bar{\gamma} \ll 1$ and $|\alpha + s| < 1$ of interest (in which the gap is guaranteed to have nodes), we have found to leading order,

$$\begin{aligned} G_0(\omega = 0) &\simeq 4iN(0)\bar{\gamma} \ln \bar{\gamma} \\ G_1(\omega = 0) &\simeq -4N(0)(\alpha + s + \delta). \end{aligned} \quad (40)$$

A. Born Limit

Using Eq. (40) in (8), in the Born limit ($c \gg 1$), we obtain

$$\bar{\gamma} \simeq e^{-\pi\tau\Delta_0} ; \quad \delta \simeq \frac{\alpha + s}{\pi\tau\Delta_0}. \quad (41)$$

Typically $\tau\Delta_0 \sim 100$ (providing the impurity concentration is low), one thus retains $\bar{\gamma} \ll 1$ and $\delta \ll |\alpha + s| < 1$. The latter validates Eqs. (26) and (28).

B. Unitary Limit

In the unitary limit ($c \ll 1$) of primary interest here, and when the resulting anisotropy is large such that $(\alpha + s)^2 \gg 1/(\tau\Delta_0)$, we found

$$\bar{\gamma} \simeq e^{-4\tau\Delta_0(\alpha+s)^2/\pi} ; \quad \delta \simeq \frac{\pi}{4\tau\Delta_0(\alpha + s)}. \quad (42)$$

Clearly Eq. (42) gives $\bar{\gamma}, \delta \ll 1$. Thus one can ignore δ in (24) to get Eqs. (26) and (28). Eq. (42) indicates that the effective scattering rate is strongly suppressed compared to isotropic case. When the resulting anisotropy is small $[(\alpha + s)^2 \lesssim 1/(\tau\Delta_0)]$, though α and $|s|$ may be large individually, the system undergoes a crossover from an anisotropic regime to a “quasi-isotropic” regime in which the gap shift δ is small and is linear in and about the size of $(\alpha + s)$. When $\alpha = -s$, δ vanishes as for a pure d -wave superconductor in an isotropic Fermi surface. More explicitly, to second order in $(\alpha + s)$, we find

$$\begin{aligned} \bar{\gamma} &\simeq \left(\frac{-\pi}{4\tau\Delta_0 \ln \bar{\gamma}_0} \right)^{\frac{1}{2}} \left[1 + \frac{2\tau\Delta_0 \ln \bar{\gamma}_0 (\alpha + s)^2}{\pi (\ln \bar{\gamma}_0 + 1)^2} \right] \\ \delta &\simeq -\frac{\alpha + s}{1 + \ln \bar{\gamma}_0}, \end{aligned} \quad (43)$$

where $\bar{\gamma}_0$ satisfies $\bar{\gamma}_0^2 \ln \bar{\gamma}_0 = -\pi/(4\tau\Delta_0)$. Typically $\ln \bar{\gamma}_0 < -2$ and with $(\alpha + s)^2 \ll 1/(\tau\Delta_0)$, the second term in the expression $\bar{\gamma}$ in Eq. (43) is small. One thus obtains a γ value similar to that for the case of a pure d -wave superconductor with an isotropic Fermi surface.

One should keep in mind that while when $(\alpha + s)^2 \ll 1/(\tau\Delta_0)$, the results for γ and δ are similar to those of an isotropic system, the universal microwave conductivities are still *anisotropic*, as given by Eq. (29). They reduce to the universal value of Eq. (25) only when $\alpha = 0$.

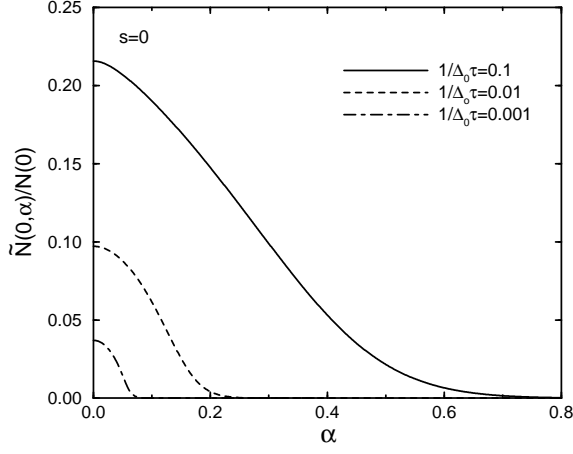


FIG. 3. Plot of zero-frequency density of states $\tilde{N}(0, \alpha)$ scaled to $N(0)$, in the unitary limit, as a function of α for different choices of scattering rate $1/\Delta_0\tau$. Here we choose $s = 0$.

C. Density of States

Using the result of (40), the impurity renormalized density of states at zero frequency is given by

$$\tilde{N}(0) = -\frac{i}{2\pi} G_0(\omega = 0) = -\frac{2N(0)}{\pi} \bar{\gamma} \ln \bar{\gamma}, \quad (44)$$

which is dependent on the impurity concentration (or $1/\tau$) and the magnitudes of α and s . In Fig. 3, we compute and plot the α dependence of $\tilde{N}(0)$, in the unitary scattering limit, for three different values of $1/(\tau\Delta_0)$, taking $s = 0$. Similar plot is made in Fig. 4 using $s = -0.25$. As already predicted for the effective scattering rate γ , the density of states is strongly suppressed when $(\alpha + s)^2 \gtrsim 1/(\tau\Delta_0)$. For example, in case of $1/(\tau\Delta_0) \sim 0.01$, $\tilde{N}(0)$ is suppressed by 50% when $(\alpha + s) \gtrsim 0.1$ compared to $(\alpha + s) = 0$ case (see Figs. 3 and 4). In comparison with experimental results, the large discrepancy between a and b -axis penetration depths [17] and normal-state resistivity [18] suggest that a large $\alpha \sim 0.4$ is required so that $\tilde{N}(0)$ is strongly suppressed. On the other hand, the low but finite-temperature universal observed value of the thermal conductivity [8] suggests that the effective scattering rate or density of states at zero frequency is not strongly suppressed. For one to be consistent with the other, it implies that a large α is accompanied by a large but negative s which reduces the effect of α and leads to less suppression of the density of states at zero frequency.

D. T_c Suppression

In the standard approach, we choose the pairing interaction to have a separable form $g(\mathbf{k}, \mathbf{k}') = -gf(\phi)f(\phi')$

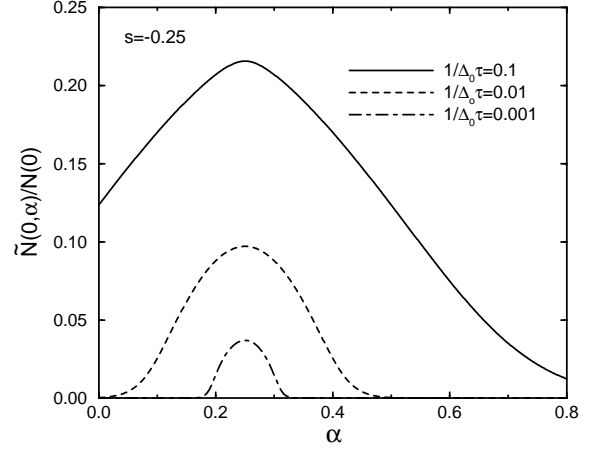


FIG. 4. Similar plot as Fig. 3 with $s = -0.25$.

($g > 0$), where $f(\phi)$ is given in (14). This reduces the gap equation of Eq. (9) to the form

$$\frac{1}{g} = 2\pi N(0)T \sum'_{\omega_n} \left\langle \frac{f(\phi)\tilde{\Delta}(\phi, \omega_n)/\Delta_0}{\sqrt{\tilde{\omega}_n^2 + \tilde{\Delta}^2(\phi, \omega_n)}} \right\rangle, \quad (45)$$

where the prime denotes a cutoff. When $T \rightarrow T_c$, it is sufficient to use the linearized version of (45), *i.e.*, ignoring the $\tilde{\Delta}$ term in denominator. In a parallel manner, one can neglect the G_1^2 term in the denominators of the self-energies in (8). This enables one to obtain, valid for both Born and unitary limits,

$$\begin{aligned} \tilde{\Delta}(\phi, \omega_n) &= \Delta_0 \left[f(\phi) + \frac{1}{2\tau} \frac{\langle f(\phi) \rangle}{|\omega_n|} \right] \\ \tilde{\omega}_n &= \omega_n + \frac{1}{2\tau} \text{sgn}(\omega_n). \end{aligned} \quad (46)$$

The second line of (46) is identical to the solution for the normal state, as expected. Thus using (46), the linearized version of (45) is reduced to

$$\frac{1}{g} = 4\pi N(0)T \sum'_{n \geq 0} \frac{\langle f^2(\phi) \rangle + \frac{1}{2\tau\omega_n} \langle f(\phi) \rangle^2}{\omega_n + \frac{1}{2\tau}}. \quad (47)$$

We have found quite generally

$$\begin{aligned} \ln \left(\frac{T_c}{T_{c0}} \right) &= \frac{\langle f^2(\phi) \rangle - \langle f(\phi) \rangle^2}{\langle f^2(\phi) \rangle} \\ &\times \left[\psi \left(\frac{1}{2} \right) - \psi \left(\frac{1}{2} + \frac{1/2\tau}{2\pi T_c} \right) \right], \end{aligned} \quad (48)$$

where T_{c0} is critical temperature in the pure case.

In our case [see (14)],

$$\begin{aligned} \langle f^2(\phi) \rangle &= \frac{1 - \sqrt{1 - \alpha^2}}{\alpha^2} (1 + 2\alpha s) + s^2 \\ \langle f(\phi) \rangle &= \frac{1 - \sqrt{1 - \alpha^2}}{\alpha} + s \end{aligned} \quad (49)$$

and to leading order, $(\langle f^2 \rangle - \langle f \rangle^2)/\langle f^2 \rangle = (2 - \alpha^2)/[2 + 4s(\alpha + s)]$. When $1/2\tau \ll T_{c0}$, we have obtained using (48)

$$\frac{T_c}{T_{c0}} = 1 - \left[\frac{2 - \alpha^2}{2 + 4s(\alpha + s)} \right] \frac{\pi}{8\tau T_{c0}}, \quad (50)$$

which depends linearly on the impurity concentration. When $1/2\tau \gg T_{c0}$, we obtain

$$\frac{T_c}{T_{c0}} = \left(\frac{1}{4\pi\tau T_{c0}} \right)^{-\left[\frac{2 - \alpha^2}{2 + 4s(\alpha + s)} \right]}. \quad (51)$$

It is shown clearly in Eqs. (50) and (51) that, in contrast to the cylindrical Fermi surface and pure d -wave gap case ($\alpha = s = 0$) in which T_c is strongly suppressed compared to T_{c0} , the presence of anisotropy (finite α or s case) reduces the effect of the suppression of T_c .

VI. CONCLUSIONS

In this paper, we have studied the low-temperature microwave conductivity and thermal conductivity for a $d_{x^2-y^2}+s$ -wave superconductor with an orthorhombic elliptical Fermi surface. Similar to the universal behaviors found in the microwave conductivity [6] and thermal conductivity [7] for a $d_{x^2-y^2}$ -wave superconductor with a cylindrical Fermi surface, *anisotropic* universal features are found in the present case. The effects of Fermi surface orthorhombicity and additional s component to the gap on the penetration depth, impurity induced T_c suppression, and the zero-frequency density of states are also considered. It is found that, compared to the cylindrical Fermi surface and pure $d_{x^2-y^2}$ -wave gap case, a small amount of anisotropy (either band anisotropy or gap admixture) will lead to a strong suppression of effective scattering rate and thus the density of states at zero frequency. Nevertheless, experimental data suggests that a large band structure anisotropy effect is compensated by a large but negative s -wave gap component.

ACKNOWLEDGMENTS

We thank Ewald Schachinger and Božidar Mitrović for stimulating discussion and May Chiao for sending us thermal conductivity results prior to publication. This work was supported in part by Natural Sciences and Engineering Research Council (NSERC) of Canada, Canadian Institute for Advanced Research (CIAR), and by National Science Council (NSC) of Taiwan under Grant No. NSC 87-2112-M-003-014.

- [1] S. L. Cooper and K. E. Gray, in *Physical Properties of High Temperature Superconductors IV*, edited by D. M. Ginsberg (World Scientific, Singapore, 1994), p. 61.
- [2] A. G. Sun *et al.*, Phys. Rev. Lett. **72**, 2267 (1994); Phys. Rev. B **54**, 6734 (1996).
- [3] K. A. Kouznetsov *et al.*, Phys. Rev. Lett. **79**, 3050 (1997).
- [4] R. Kleiner *et al.*, Phys. Rev. Lett. **76**, 2161 (1996).
- [5] H. Aubin, K. Behnia, M. Ribault, R. Gagnon, and L. Taillefer, Phys. Rev. Lett. **78**, 2624 (1997).
- [6] P. A. Lee, Phys. Rev. Lett. **71**, 1887 (1993).
- [7] M. J. Graf, S.-K. Yip, J. A. Sauls, and D. Rainer, Phys. Rev. B **53**, 15147 (1996).
- [8] L. Taillefer, B. Lussier, R. Gagnon, K. Behnia, and H. Aubin, Phys. Rev. Lett. **79**, 483 (1997).
- [9] W. C. Wu and J. P. Carbotte, Phys. Rev. B **57**, R5614 (1998).
- [10] D. N. Basov *et al.*, Phys. Rev. Lett. **74**, 598 (1995).
- [11] M. Chiao *et al.*, to be published.
- [12] S. B. Nam, Phys. Rev. **156**, 470 (1967).
- [13] H. Kim and E. J. Nicol, Phys. Rev. B **52**, 13576 (1995).
- [14] P. J. Hirschfeld, W. O. Putikka, and D. J. Scalapino, Phys. Rev. Lett. **71**, 3705 (1993); Phys. Rev. B **50**, 10250 (1994).
- [15] D. Tanner *et al.*, SPIE **2696**, 13 (1996).
- [16] D. Tanner and T. Timusk, in *Physical Properties of High Temperature Superconductors III*, edited by D. M. Ginsberg (World Scientific, Singapore, 1992), p. 363.
- [17] D.A. Bonn, S. Kamal, K. Zhang, R. Liang, W.N. Hardy, J. Phys. Chem. Solids **56**, 1941 (1995).
- [18] K. Zhang *et al.*, Phys. Rev. Lett. **73**, 2484 (1994).
- [19] I. Schürer, E. Schachinger, and J.P. Carbotte, preprint.